INVESTIGATION OF SELF-CLEANING PROPERTIES OF COTTON FABRICS BY *IN SITU* SYNTHESIS NANO-TiO_2 USING DIFFERENT PRECURSORS

SHEILA SHAHIDI,[*] SHABNAM ANDALIB,[**] ZAHRA MOTAGHI,[***] RATTANAPHOL MONGKHOLRATTANASIT[****] and EMADALDIN HEZAVEHI[*]

[*]*Department of Textiles, Arak Branch, Islamic Azad University, Arak, Iran*
[**]*Plasma Physics Research Center, Science and Research Branch, Islamic Azad University, Tehran, Iran*
[***]*Department of Textiles, Sabzevar Branch, Islamic Azad University, Sabzevar, Iran*
[****]*Department of Textile Chemistry Technology, Rajamangala University of Technology Phra Nakhon, Faculty of Industrial Textiles and Fashion Design, Bangkok, Thailand*
✉ *Corresponding author: R. Mongkholrattanasit, rattanaphol.m@rmutp.ac.th*

Received November 9, 2023

Surface modification is a special feature in the textile industry. The end use performance of a textile product is greatly influenced by its final properties. A new concept has been developed based on the 'lotus leaf' principle, namely, 'self-cleaning textiles', *i.e.* textile surfaces that can clean themselves, without any washing process. The use of superfine materials made by means of nanotechnologies has received attention in the process of finishing textiles in recent years. Nanomaterials or nanoscale nanomaterials are used to endow textiles with various properties, such as radiation resistance, antimicrobial properties, self-cleaning, amortization, and others. In this study, titanium dioxide nanoparticles were simultaneously sono-synthesized and coated onto cotton fabric. For the synthesis of titanium dioxide nanoparticles, two different precursors, namely, titanium isopoxide (TTIP) and titanium butoxide (TTIB) have been used. Several analytical methods, including field emission scanning electron microscopy (FESEM), scanning electron microscopy (SEM), X-ray diffraction (XRD), energy dispersive X-ray (EDX), dynamic light scattering (DLS), ultraviolet visible (UV-Vis) spectroscopy, were used to confirm the presence of TiO_2 nanoparticles and investigate the self-cleaning property of treated fabrics.

Keywords: titanium dioxide nanoparticles, sono-synthesis, anatase, titanium isopoxide (TTIP), titanium butoxide (TTIB)

INTRODUCTION

Nanotechnology has revolutionized the textile industry by enabling the development of materials with novel properties that were previously unattainable. Among these advancements, the application of nanostructures, such as silver, silicon dioxide, titanium dioxide, zinc oxide, carbon nanotubes, copper oxides, gold, and iron, has become increasingly prominent due to their ability to impart unique functionalities to fabrics. In particular, titanium dioxide (TiO_2) and zinc oxide nanoparticles have been widely utilized due to their self-cleaning capabilities, and their demand on the global market continues to grow rapidly.[1-6]

Self-cleaning textiles, which can remove dirt and stains without traditional washing, have garnered significant interest for their potential applications in various industries. This functionality can be achieved through two main mechanisms: hydrophobic surfaces that repel water and contaminants, and hydrophilic surfaces that facilitate contaminant breakdown via photocatalysis. Both methods rely on modifying the fabric's surface properties to enhance resistance to liquid penetration, such as ink, beverages, and blood, thereby reducing the frequency and cost of washing.[3-6]

Nanoparticles, such as titanium dioxide (TiO_2) offer dual benefits by providing self-cleaning

properties through photocatalytic activity and potentially improving other fabric characteristics, such as durability, UV resistance, and antimicrobial effects. TiO_2, in particular, is a widely used metal oxide due to its high photocatalytic activity, chemical stability, and cost-effectiveness. The photocatalytic properties of TiO_2, especially in its anatase crystalline phase, allow it to break down organic contaminants upon exposure to ultraviolet (UV) light. This process is facilitated by the generation of reactive oxygen species (ROS), which degrade organic materials, leading to a self-cleaning effect.[6-10]

Recent studies have demonstrated that self-cleaning textiles treated with TiO_2 nanoparticles offer several advantages over those treated with traditional hydrophobic methods. These benefits include greater durability, enhanced multi-functionality (*e.g.*, antibacterial, anti-odor, and UV-absorbent properties), and improved environmental stability. However, the effectiveness of TiO_2 coatings is influenced by the synthesis method, particle size, surface modifications, and doping elements. Therefore, optimizing the synthesis method is crucial to maximising the self-cleaning efficiency of these nanomaterials.

Several synthesis methods have been explored for producing TiO_2 nanoparticles, such as mechano-chemical methods, thermal plasma processes, chemical vapour condensation, and micro-mixing techniques.[11-21] This study focuses on an *in situ* sono-synthesis method to simultaneously synthesize and coat TiO_2 nanoparticles onto cotton fabric. Using two different precursors, titanium isopropoxide (TTIP) and titanium butoxide (TTIB), this approach aims to evaluate the self-cleaning efficiency and characterize the resulting nanostructures' properties on the fabric.

The objective of this research is to investigate the self-cleaning properties of cotton fabrics treated with *in situ* synthesized TiO_2 nanoparticles. By comparing different synthesis conditions and precursors, this study seeks to optimize the application of TiO_2 nanoparticles for enhanced self-cleaning functionality, while maintaining or improving the fabric's other essential properties.

EXPERIMENTAL

Materials

Desized, scoured, and bleached plain weave 100% cotton fabric, with 36 and 26 wefts/cm, was supplied by Momtaz Fabrics Company (Tehran, Iran). Titanium tetra isopropoxide (97%, TTIP) and titanium butoxide (97%, TTIB) were purchased from Merck, Germany. Acetic acid 100%, hydrochloric acid 37%, ethanol and methylene blue (MB) hydrate (>70%) were also received from Merck, Germany.

Sample preparation

Two preparation methods were used in this work. In the first method, to perform the *in situ* sonosynthesis of TiO_2 nanoparticles, 100 mL of distilled water was mixed with 0.2 mL of acetic acid using a magnetic stirrer at 250 rpm for 5 minutes. A 5 × 5 cm^2 piece of cotton fabric was immersed in the prepared solution and sonicated in an ultrasonic bath, using an ultrasonic processor (Model 100; Sonic, USA) and the solution was kept under low-frequency (25 kHz) ultrasonic irradiation for 5 minutes. Subsequently, 3 mL of titanium tetra isopropoxide (TTIP) was added dropwise to the solution during sonication. The mixture was sonicated for 2 hours under ambient conditions. After the treatment, the fabric was kept at 25 °C for 24 hours, thoroughly washed with distilled water, and then dried again at ambient temperature. To optimize the self-cleaning properties, the concentration of the TTIP precursor was varied to 2 mL and 1 mL in subsequent samples.

In the second method, 40 mL of ethanol was mixed with 60 mL of distilled water and 0.15 mL of HCl using a magnetic stirrer set at 250 rpm for 5 minutes. A 5 × 5 cm^2 piece of cotton fabric was immersed in the prepared solution and sonicated in an ultrasonic bath under low-frequency (25 kHz) ultrasonic irradiation for 5 minutes. During sonication, 3 mL of titanium butoxide (TTIB) was added dropwise to the solution. The mixture was sonicated for 2 h at 60 °C. After treatment, the fabric was kept at 25 °C for 24 hours, thoroughly washed with distilled water, and dried again at ambient temperature. Similar to the first method, the concentration of the TTIB precursor was adjusted to 2 mL and 1 mL in subsequent samples to determine the optimal conditions for enhancing the self-cleaning properties of the fabric.

Characterization methods

The morphology of the TiO_2 nanoparticles and the treated cotton fabrics was observed using a field-emission scanning microscope (TESCAN MIRA3-XMU FE-SEM, made in Czech Republic) with magnifications of 2000x and 10,000x. Additional imaging was performed using a scanning electron microscope (SEM, EM3200, Kyky, China). The crystallinity and structural properties of the synthesized TiO_2 nanoparticles were characterized using an X-ray diffractometer (PANalytical X'pert Pro MPD XRD system, Netherlands), equipped with Cu-Kα radiation at 40-60 kV and 200 mA. The particle size distribution of treated samples was determined

using dynamic light scattering (DLS) with a Nano ZS (Red Badge) ZEN 3600 instrument (Malvern, UK).

The optical properties of the photo-catalyst treated cotton samples were evaluated by measuring the reflection factor from 460 nm to 760 nm using a spectrophotometer (Ultrascan XE, Hunter Lab, USA), which is capable of analyzing a wide range of electromagnetic waves in the UV-Vis-NIR range (175 nm-3300 nm). Diffuse Reflectance Accessory (DRA) analysis was also utilized in this study. The self-cleaning performance was assessed using a custom-made setup equipped with a UV lamp (Hitachi, Japan) with 15 watts of power. Fabric samples were immersed in 5 mL of 0.01% methylene blue solution, and the dyed fabrics were exposed to UV light for 12 hours after drying, to compare their color reduction and self-cleaning. After visual comparison of the decolorization of the fabrics, their reflectance spectra were compared, with using reflective spectroscopy, to examine their self-cleaning ability.

RESULTS AND DISCUSSION

Scanning electron microscopy (SEM)

SEM analysis was employed to observe the morphology of the samples and determine the size of nanoparticles. Several solutions containing titanium dioxide nanoparticles, prepared using TTIP and TTIB precursors at different concentrations, were subjected to SEM analysis. SEM analysis was performed to observe the morphology of the samples and determine the size of the nanoparticles. A certain amount of the samples was dried on glass slides and prepared for imaging.

SEM images were recorded for three samples of TiO_2 nanoparticles synthesized from TTIP with the following concentrations: 3 mL (sample 1), 2 mL (sample 2) and 1 mL (sample 3), as well as for three samples TiO_2 nanoparticles synthesized from TTIB, with concentrations of 3 mL (sample 4), 2 mL (sample 5) and 1 mL (sample 6).

SEM images obtained from TiO_2 nanoparticles prepared with 3 different concentrations of titanium tetra isopropoxide (TTIP) precursor are shown in Figure 1. As can be seen, TiO_2 nanoparticles have a spherical shape and are almost uniform. The average size of the nanoparticles was calculated, and it was found that, with the changes in concentration, the average particle size remained almost constant.

The size distribution of the nanoparticles below 100 nm synthesized from TTIP was determined and shown in Figure 2. According to Figure 2 (a), the average nanoparticle size in sample 1 is approximately 75 nm, in sample 2, it is approximately 88 nm (Fig. 2 (b)), and in sample 3, the average nanoparticle size is approximately 80 nm (Fig. 2 (c)). The smallest TiO_2 nanoparticles are identified as sample 1. Thus, the best result in this group was achieved with a concentration of 3 mL of TTIP precursor.

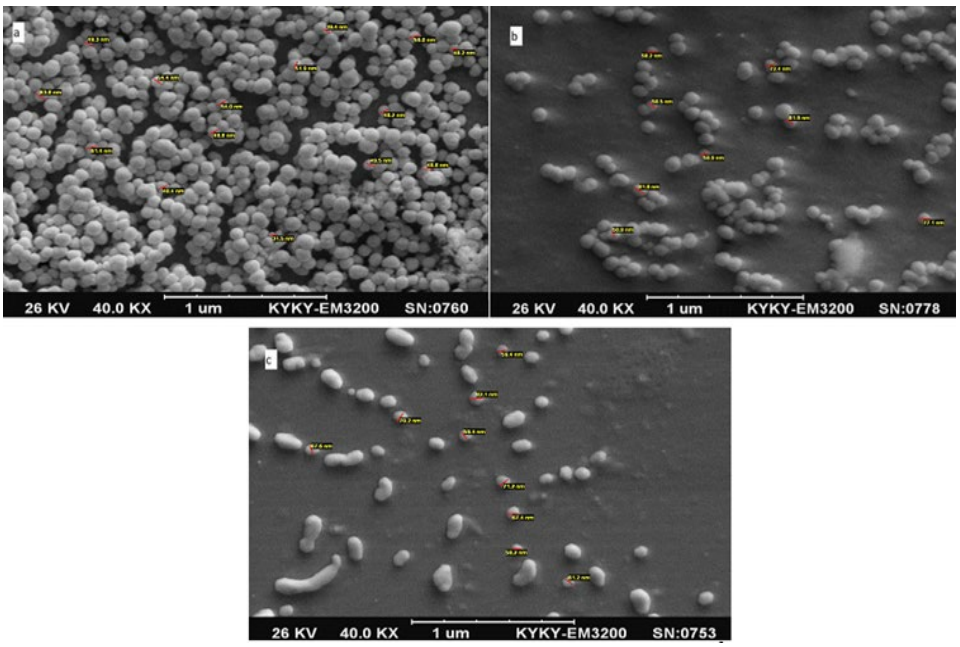

Figure 1: SEM images of TiO_2 nanoparticles synthesized from TTIP with an average nanoparticle size of (a) Sample 1 – 50 nm; (b) Sample 2 – 64 nm; (c) Sample 3 – 60 nm

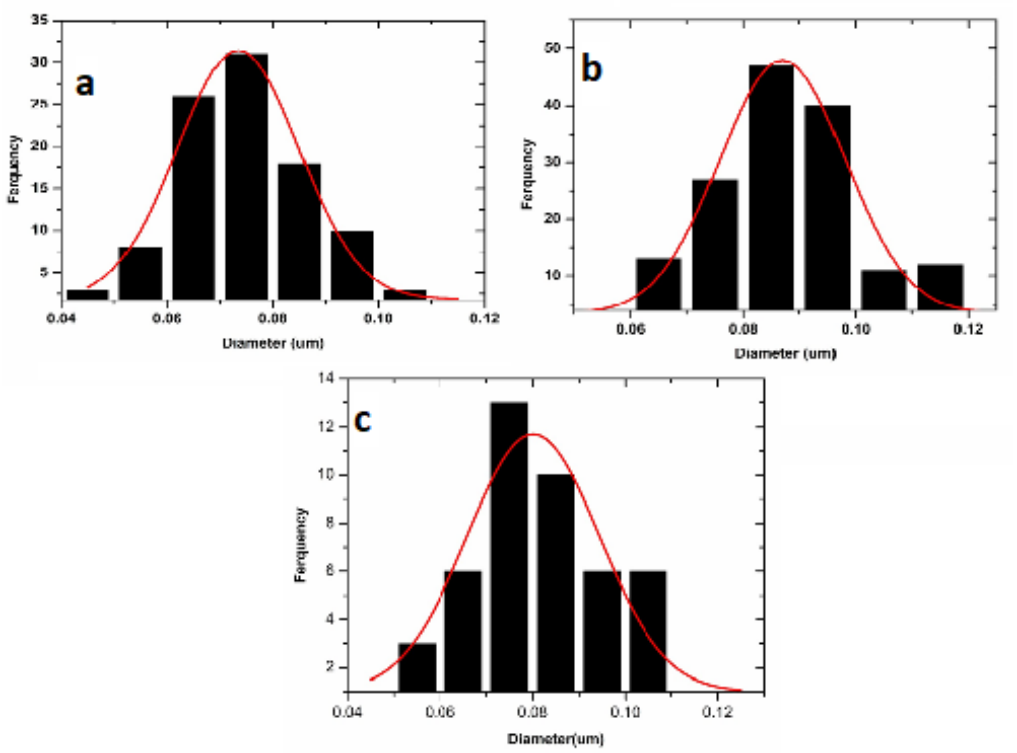

Figure 2: Histogram of size distribution of nanoparticles below 100 nm; (a) Sample 1, (b) Sample 2, and (c) Sample 3

A comparison of SEM images for the samples of TiO_2 nanoparticles prepared with three different concentrations (samples 4, 5 and 6) of titanium butoxide (TTIB) precursor is shown in Figure 3. SEM images reveal the spherical and almost uniform appearance of TiO_2 nanoparticles. The average particle size of the nanoparticles was calculated and it was determined that it did not change significantly with concentration. Figure 4 shows the distribution of nanoparticle sizes below 100 nm, and the average nanoparticle size is approximately 78 nm for sample 4 (Fig. 4 (a)), it is approximately 80 nm for sample 5 (Fig. 4 (b)), and approximately 80 nm for sample 6 (Fig. 4 (c)). Sample 4 contained the smallest TiO_2 nanoparticles. Thus, the best result in this group was achieved using a concentration of 3 mL of TTIB precursor. Although the particles in both groups had an average size that was almost identical, the sample obtained with a concentration of 3 mL of precursor achieved the smallest size.

Field emission scanning electron microscopy (FESEM)

FESEM analysis was used to investigate the morphology of the fabric samples and confirm the presence of titanium dioxide nanoparticles on the fabric surface. Cotton fabrics coated with titanium dioxide nanoparticles using TTIP and TTIB precursors were subjected to FESEM analysis. Images were taken to compare the distribution of nanoparticles on six different samples of coated fabrics at varying concentrations.

Figure 5 shows the FESEM images of the fabric surface coated with TiO_2 nanoparticles at three different concentrations of titanium tetra isopropoxide (TTIP) precursor, while the image of the untreated raw cotton fabric reveals a clean surface, free from nanoparticles or other impurities. Also, these images, taken at the same magnifications as those used in SEM analysis, show that, even after washing, the nanoparticles remain adhered to the fabric surface.

Figure 6 presents the FE-SEM images of fabric samples coated with TiO_2 nanoparticles synthesized using the TTIB precursor via sonication and *in situ* synthesis. The surface appears to be uniformly coated with nanoparticles.

Samples 5 and 6 show a lower density of nanoparticles compared to the previous images, though no significant difference in surface coverage is observed. FE-SEM images reveal that the nanoparticles are less uniformly shaped on the fabric surface than in the SEM images, where

nanoparticles were deposited on glass slides. This suggests that TiO_2 nanoparticle aggregation occurs more readily on the cotton fabric surface than on smooth glass surfaces. The results from SEM and FE-SEM images, as well as those from the histograms indicate that the TTIP precursor was more effective in achieving uniform nanoparticle size and distribution.

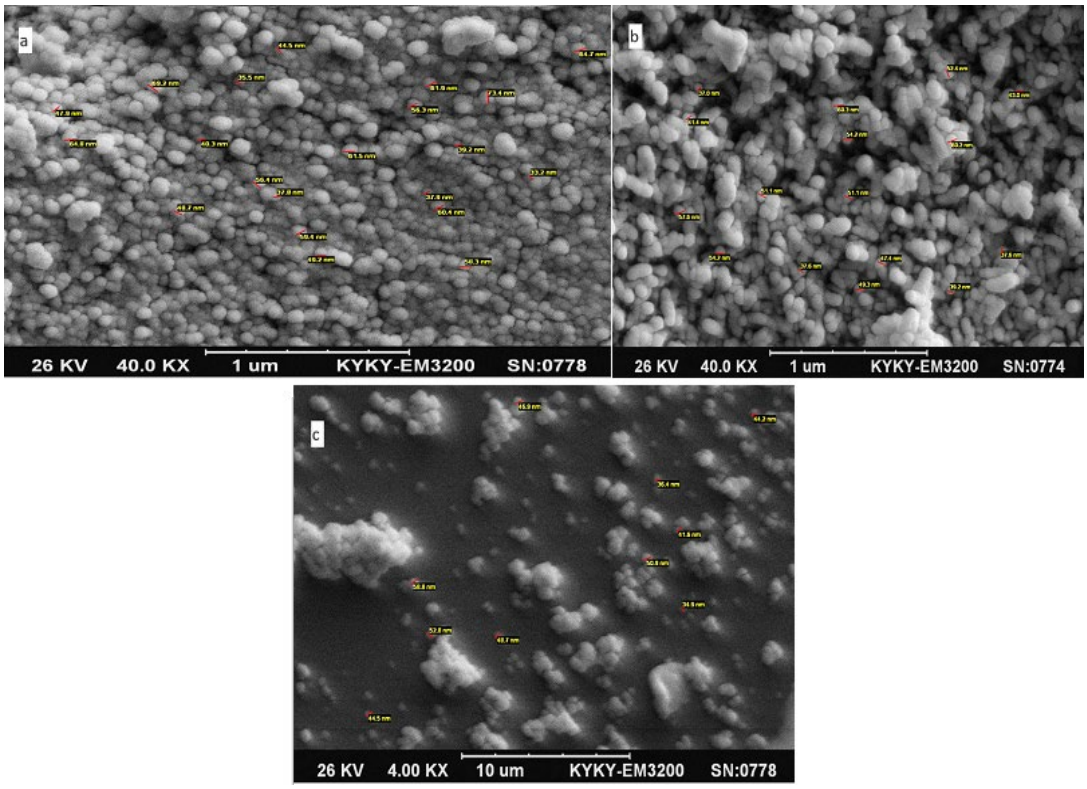

Figure 3: SEM images of TiO_2 nanoparticles synthesized from TTIB precursor, with an average nanoparticle size of (a) Sample 4 – 53 nm, (b) Sample 5 – 55nm, (c) Sample 6 – 52 nm

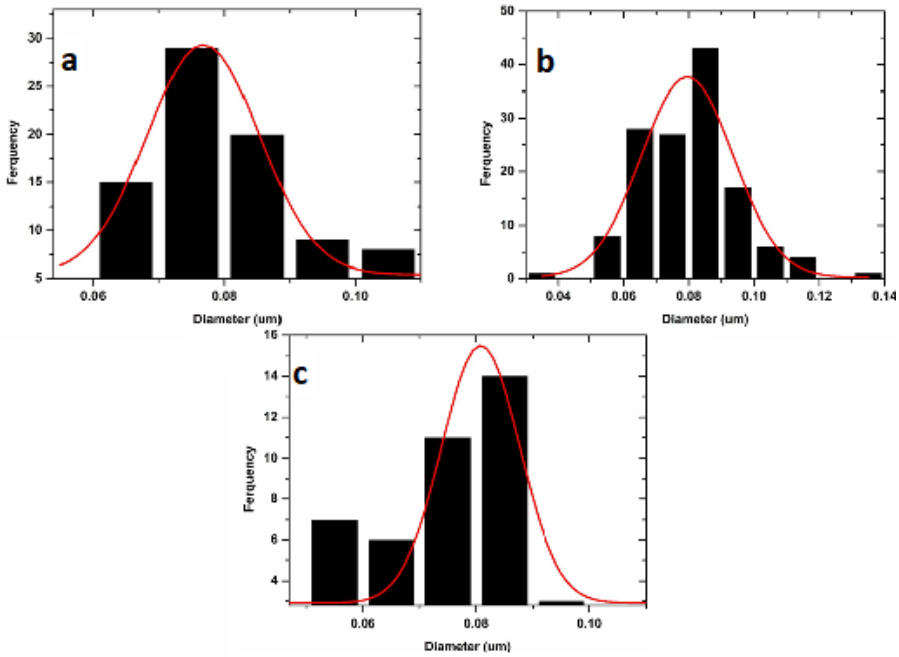

Figure 4: Histogram of size distribution of nanoparticles below 100 nm, (a) sample 4, (b) sample 5, (c) sample 6

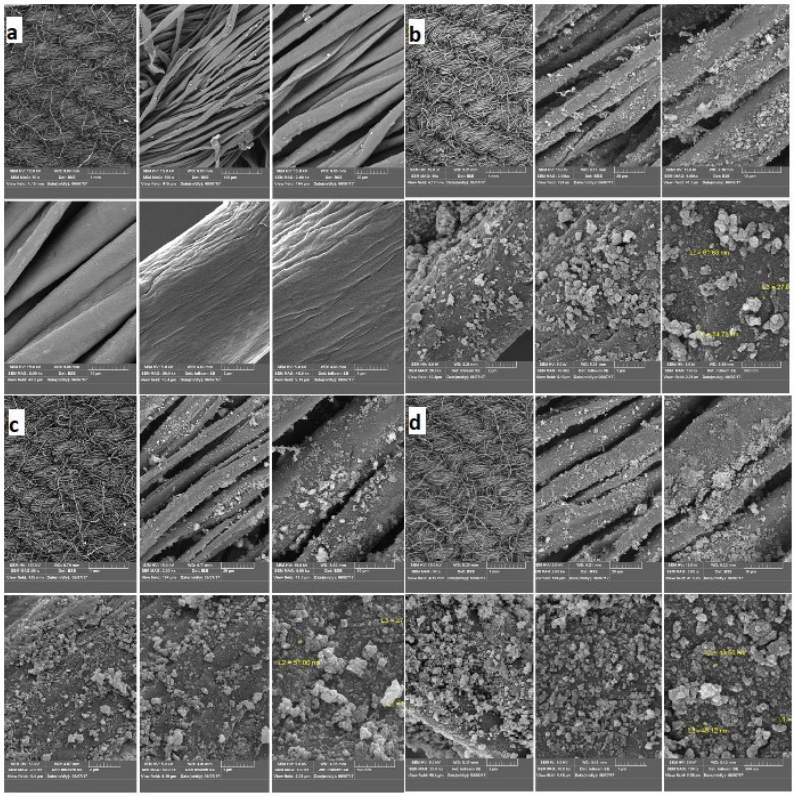

Figure 5: FE-SEM images of raw cotton fabric (a), and of fabrics coated with TiO_2 nanoparticles by the *in situ* synthesis method, (b) sample 1, (c) sample 2, (d) sample 3, at magnifications of 50X, 500X, 2.00KX, 5.00KX, 20.0KX and 40.0KX

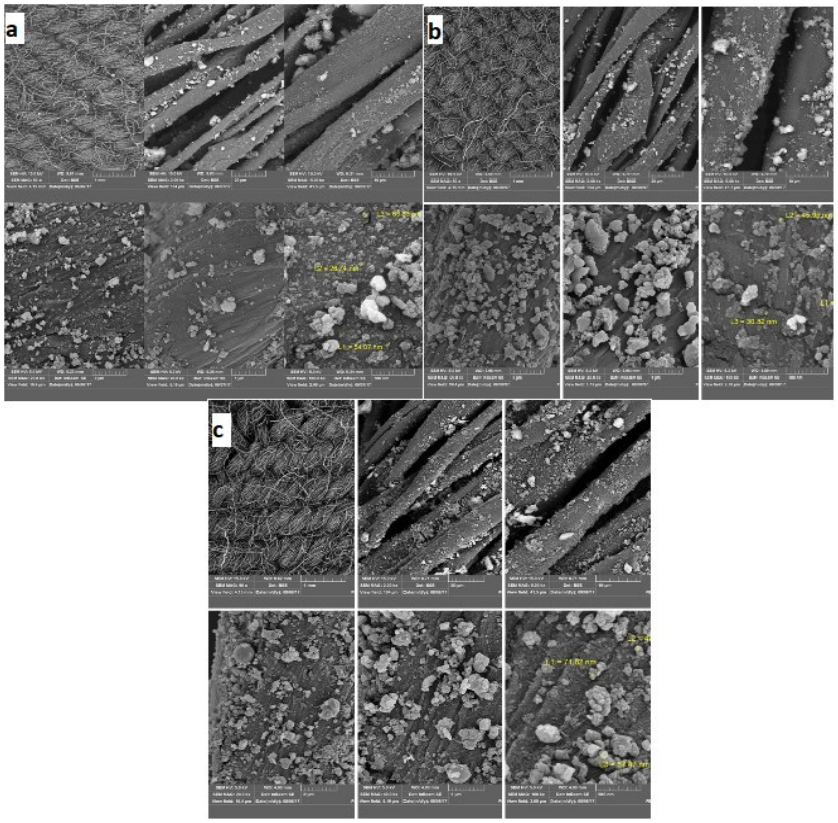

Figure 6: FE-SEM images of fabric coated with TiO2 nanoparticles by *in situ* synthesis method, (a) sample 4, (b) sample 5, (c) sample 6, at magnifications of 50X, 500X, 2.00KX, 5.00KX, 20.0KX and 40.0KX

EDX spectroscopy

Energy dispersive X-ray spectroscopy (EDX) was used to determine the elemental composition of the TiO_2 nanoparticles and confirm their successful deposition on the cotton fabrics. This technique was performed on TiO_2 coated fabrics, synthesized using both TTIP and TTIB precursors, to compare their elemental composition. The results are presented in Figures 7 and 8, and in Tables 1 and 2.

EDX analysis was conducted on fabric samples coated with TiO_2 nanoparticles synthesized using the TTIP and TTIB precursors at concentrations of 3 mL. The EDX spectra (Figs. 7 and 8) show distinct peaks corresponding to titanium (Ti) and oxygen (O), confirming the presence of TiO_2 nanoparticles on the fabric surfaces. The weight percentages of titanium detected were approximately 13.63% and 12.56%, for the 3 mL concentrations of TTIP and TTIB precursors, respectively. These results indicate that the weight percentage of the titanium element for the TTIB precursor is lower than that of the TTIP precursor.

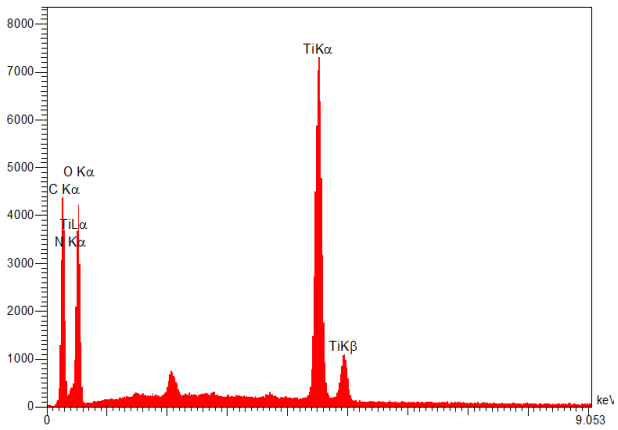

Figure 7: EDX spectrum of fabric coated with TiO_2 nanoparticles (TTIP 3 mL)

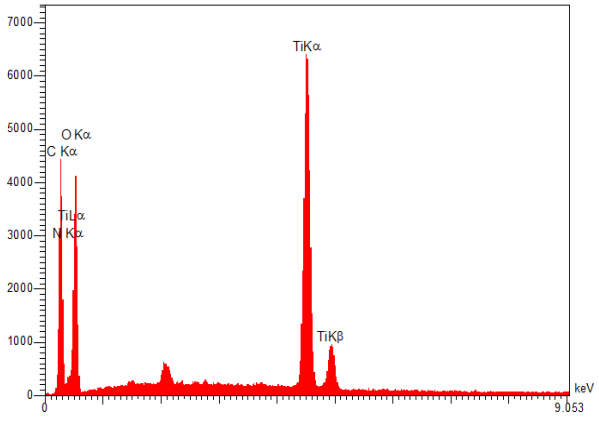

Figure 8: EDX spectrum of fabric coated with TiO_2 nanoparticles (TTIB 3 mL)

Table 1
EDX results of fabrics coated with TiO_2 nanoparticles (TTIP 3 mL)

Element	Weight percentage (wt%)	Atomic percentage (A%)
C	32.2	41.55
N	7.68	8.55
O	46.67	45.47
Ti	13.63	4.44

Table 2
EDX results of fabrics coated with TiO_2 nanoparticles (TTIB 3 mL)

Element	Weight percentage (wt%)	Atomic percentage (A%)
C	33.37	42.81
N	7.82	8.60
O	46.25	44.54
Ti	12.56	4.04

Comparing the EDX analysis data presented in Figures 7 and 8 and in Tables 1 and 2, it was found that the weight percentage of the titanium element was lower when using the TTIB precursor than in the case of the TTIP precursor.

XRD (X-ray diffraction) analysis

Samples of solutions containing titanium dioxide nanoparticles synthesized using the two precursors, TTIP and TTIB, with concentrations of 3 mL, were subjected to XRD analysis. For this

purpose, the samples of the solutions were dried, and XRD analysis of the powder samples was performed to detect the crystal phase, the crystallite size and the geometry of the crystal lattice.

The XRD pattern related to TiO_2 nanoparticles synthesized from the TTIP precursor is shown in Figure 9. In the XRD pattern, a series of characteristic peaks were observed at 2θ angles equal to 75.31°, 69.50°, 62.87°, 54.51°, 47.86°, 38.09° and 25.46°, which indicate the inclusion of the pure anatase (tetragonal crystal) structure, in accordance with 98-010-6863 standard card.

The XRD pattern of the TiO_2 nanoparticle sample synthesized using the TTIB precursor is shown in Figure 10. According to the XRD pattern, a series of characteristic peaks were observed at 2θ angles equal to 75.55°, 69.5°, 62.88°, 54.60°, 47.75°, 37.96° and 25.37°, which indicate the inclusion of the pure anatase structure (tetragonal crystal), in accordance with the 98-010-6863 standard card.

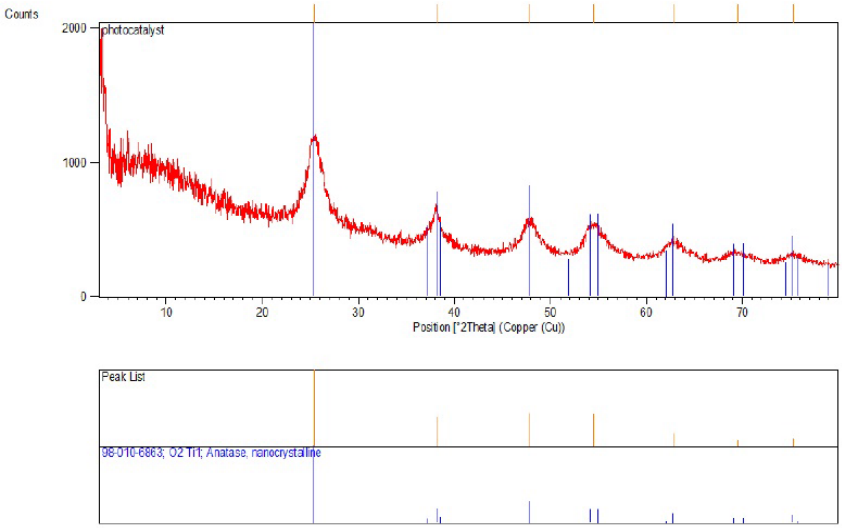

Figure 9: XRD pattern of TiO_2 nanoparticle powder sample synthesized from 3 mL of TTIP precursor

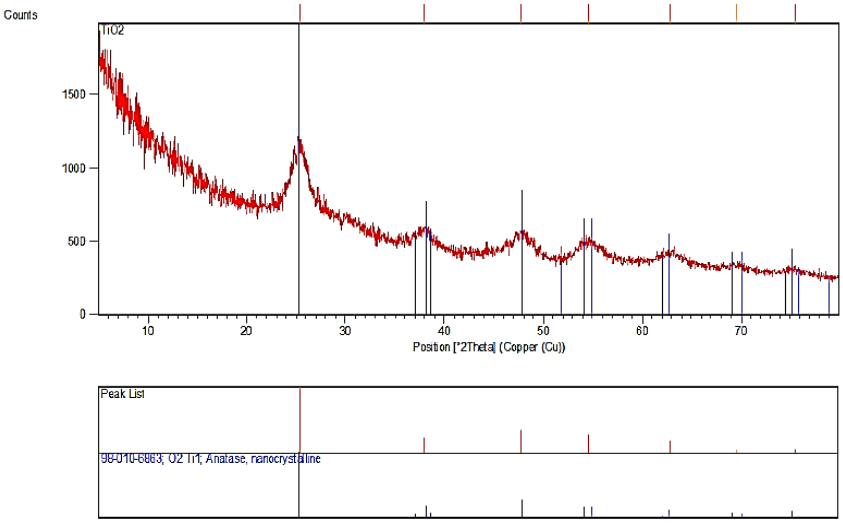

Figure 10: XRD pattern of TiO_2 nanoparticle powder sample synthesized from 3 mL of TTIB precursor

Table 3
Crystallite sizes of TiO_2 nanoparticles

Sample	FWHM (2Th.)	2θ	D (Å)
TiO_2 (TTIP)	2.215	25.37	37
TiO_2 (TTIB)	1.765	25.46	46

The crystallite size of TiO_2 nanoparticles was calculated using the Debay-Scherer equation:

$$D = \frac{K\lambda}{\beta \cos\alpha} \quad (1)$$

where: D – size of nanoparticle crystallite in nm, λ: wavelength for kα anode of the device equal to 0.154 nm, β: peak width at half the height of the maximum (or FwHm) in terms of radians, θ: location of the peak on the horizontal axis of the diffraction pattern (the angle between the radiation beam and the reflection) which, if 2 on the horizontal axis, must be divided by 2 to obtain θ. The results obtained were listed in Table 3.

The crystallite size of TiO_2 nanoparticles synthesized from both precursors is about 4 nm. Similar data were obtained by both Expert software and Debbie-Scherer formula. It should be noted that the XRD method provides the grain size, and not the particle size. Therefore, usually, the SEM and DLS results are several times greater than those yielded by XRD, unless the particle is obtained from one grain. Also, the results achieved for the crystallite size of TiO_2 nanoparticles obtained from both precursors are the same.

Particle size distribution by DLS

Dynamic light scattering (DLS) is one of the recommended methods for determining the particle size distribution. In this method, the distribution of particle dimensions in a solution can be determined from the orthogonal motion of the particles in the fluid. Two solutions containing titanium dioxide nanoparticles, one prepared with 3 mL of TTIP precursor and the other prepared with 3 mL of TTIB precursor, were subjected to DLS analysis to distribute their particle size according to volume, number of particles and light intensity scattered. The results of SEM and FESEM are not related to the particle size distribution. The analysis is limited to determining the size of a small number of particles. DLS analysis is required to generalize the particle size to the total manufactured particles, as the results are statistically much more relevant than microscopic images. Therefore, DLS is needed as an additional tool to microscopy images.

Figures 11 and 12 show the particle size distribution diagrams in the DLS device in three forms of scattered light intensity, volume and number, for two solution samples containing TiO_2 nanoparticles. Since, in some experiments, particle size distribution in terms of number or volume of particles is required, the particle size distribution diagram in terms of scattered light intensity must be converted to a particle size distribution diagram in terms of volume and number. In these diagrams, the X-axis is the particle size distribution and the Y-axis shows the relative intensity of light scattering or the volume or number of particles.

Comparing Figures 11 and 12, it can be concluded that the area under the particle size distribution by intensity curve of TTIB precursor is almost twice as much as that corresponding to the TTIP precursor. In the particle distribution diagram by volume, the peak of TiO_2 nanoparticles synthesized with titanium butoxide precursor is higher than that of nanoparticles synthesized with TTIP, indicating that the particles with propoxide precursor are smaller. Because volume is directly related to the third power of the particle radius (spherical particles are assumed) in the particle distribution diagram according to light intensity, again the peak of nanoparticles with TTIP precursor is lower and the area below the diagram is smaller. Therefore, it is again concluded that the particles produced by the propoxide precursor are slightly smaller because the intensity of the scattered light is directly related to the particle size, which is (r6) in this relation. The distribution of nanoparticles in the range of 100 nm to 1000 nm is good in both samples. The particle size in the diffuser solution is larger because the dynamic light scattering method determines it. The reason for this is the existence of a double electrical layer (zeta potential) that surrounds the particle.

Ultraviolet visible (UV-Vis) spectroscopy

The ultraviolet visible absorption spectroscopy was performed according to the standard 3008-0102-7 on a highly diluted solution sample of TiO_2 nanoparticles. The absorption peak was observed in the ultraviolet range (Fig. 13).

This method can be utilized to detect TiO_2 due to the presence of specific absorption peaks in the UV-Vis spectrum. Figure 13 indicates that TiO_2 has an absorption peak in the 200-300 nm range, which is within the UV spectrum. The absorption spectrum indicates that titanium particles are present because TiO_2 nanoparticles absorb UV in the same range. Also, the reflectance spectrum (UV-Vis) was recorded using the DRA system of a spectrophotometric device for three fabric samples to compare the results. The three fabric

samples tested for this experiment were: sample 1 – the raw fabric, sample 2 – the fabric coated with TiO_2 nanoparticles (TTIP precursor 3 mL), and sample 3 – the fabric coated with TiO_2 nanoparticles (TTIB precursor 3 mL). Based on the reflectance spectra shown in Figure 14, the reflection factor for samples 2 and 3 in the wavelength range of 200-300 nm is very low (close to zero), which confirms the presence of TiO_2 nanoparticles on the cotton fabric.

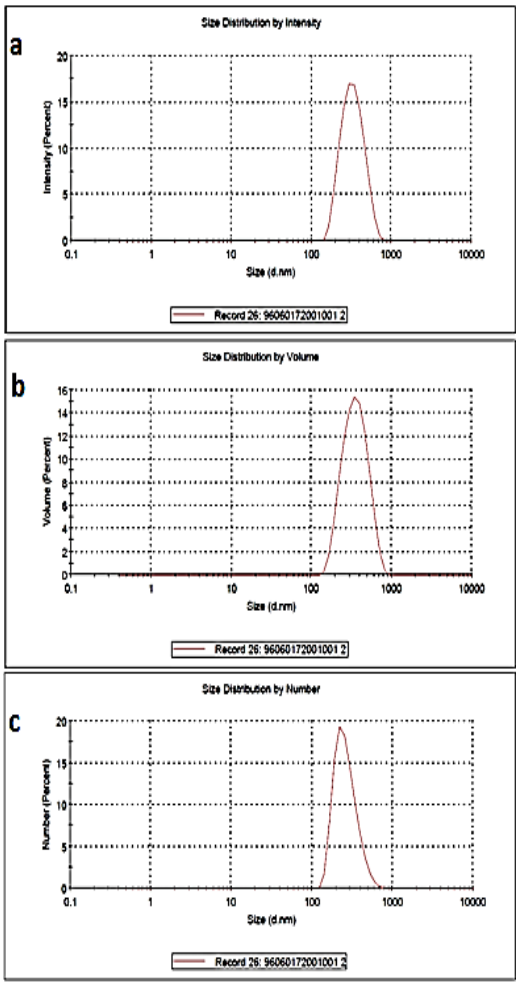

Figure 11: DLS diagrams of TiO_2 nanoparticles (TTIP 3 mL): (a) Particle size distribution according to scattered light intensity; (b) Particle size distribution in terms of volume; (c) Particle size distribution in terms of number of particles

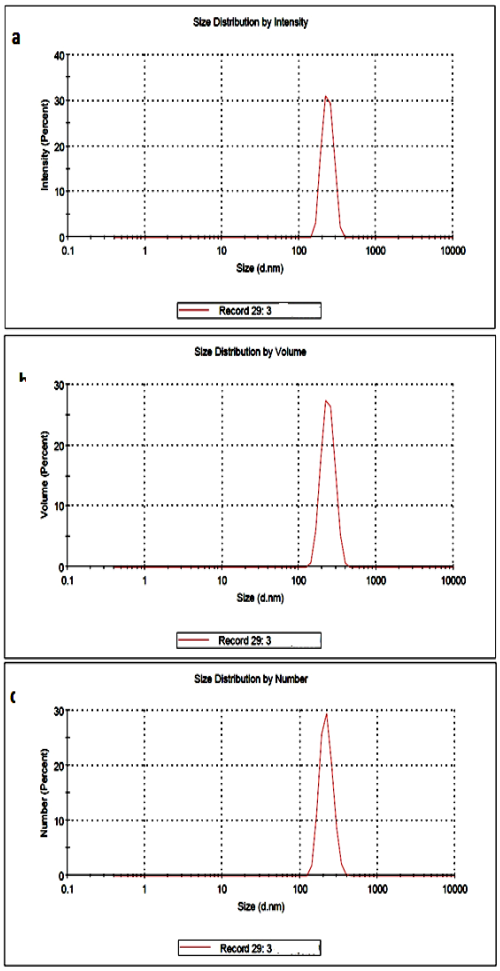

Figure 12: DLS diagrams TiO_2 nanoparticles (TTIB 3 mL): (a) Particle size distribution according to scattered light intensity; (b) Particle size distribution in terms of volume; (c) Particle size distribution in terms of number of particles

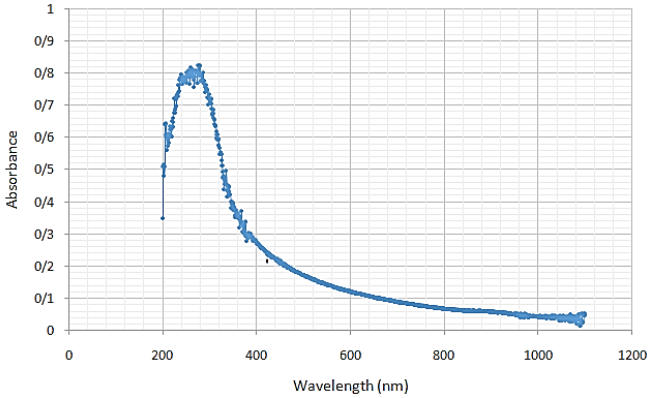

Figure 13: Absorption spectrum of a solution containing TiO_2 nanoparticles

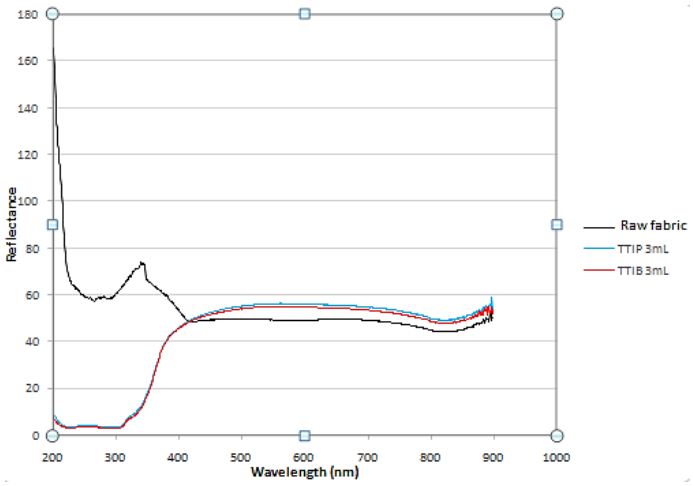

Figure 14: Reflectance spectra of fabric samples coated with TiO_2 nanoparticles

Self-cleaning properties of treated fabrics

The self-cleaning rate of the fabrics was assessed with a self-cleaning setup device provided with a UV lamp. Fabric samples, with approximate dimensions of 3×3 cm^2, were immersed in 5 mL of 0.01% methylene blue solution, and the dyed fabrics were dried at an ambient temperature of 25 °C. The samples of colored fabrics, including three samples of fabric loaded with TiO_2 nanoparticles synthesized from 3 mL, 2 mL and 1 mL of TTIP precursor, three samples of fabric loaded with TiO_2 nanoparticles synthesized from 3 mL, 2 mL and 1 mL of TTIB precursor, and a sample of raw untreated fabric, were exposed to UV light for 12 hours after drying, in order to compare their color reduction and self-cleaning property. After visual comparison of the decolorization of the fabrics, the colored fabrics were subjected to reflectance spectroscopy to compare their reflectance spectra in order to assess their self-cleaning ability.

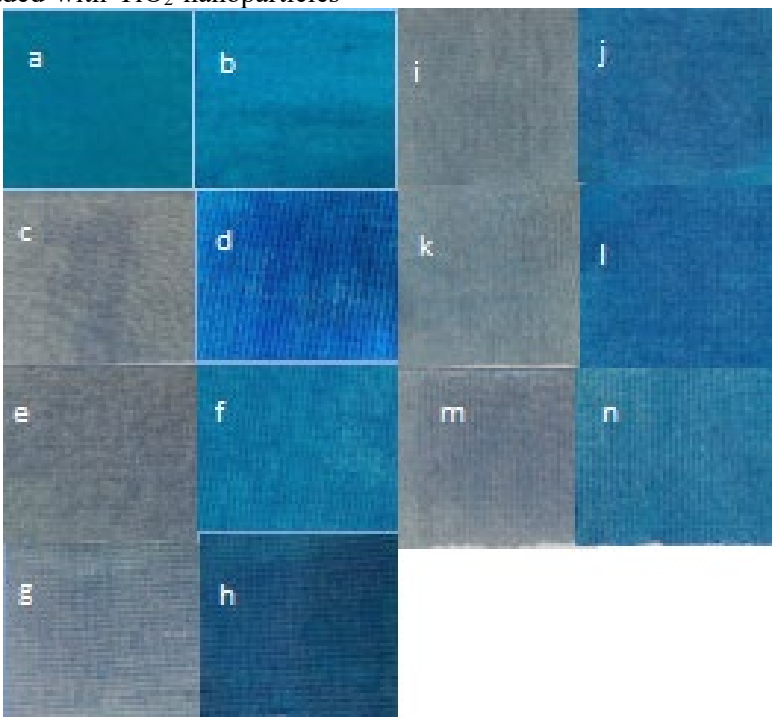

Figure 15: Images of fabrics dyed with methylene blue before (samples a, d, f, h, j, l and n) and after (samples b, c, e, g, i, k, and m) UV light irradiation for 12 hours; (a, b) raw fabrics; (c, d) samples treated with TTIP 3 mL; (e, f) samples treated with TTIP 2 mL, (g, h) samples treated with TTIP 1 mL; (i, j) samples treated with TTIB 3 mL, (k, l) samples treated with TTIB 2 mL, (m, n) samples treated with TTIB 1 mL

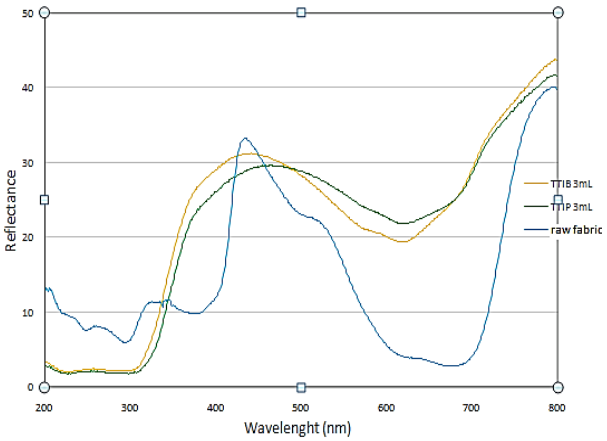

Figure 16: Reflection spectra of raw fabrics and fabrics loaded with TiO_2 nanoparticles dyed with methylene blue after exposure to UV light

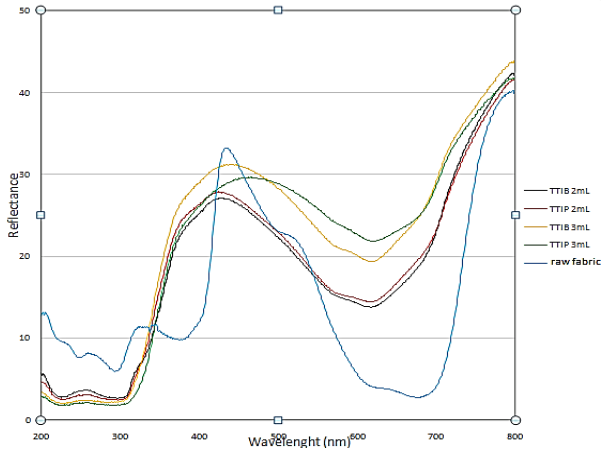

Figure 17: Reflection spectra of raw fabrics and fabrics loaded with TiO_2 nanoparticles impregnated with methylene blue

Figure 15 shows the selected fabrics, before and after irradiation for 12 hours, and revealing the decomposition of methylene blue within the samples.

Visual comparison of the images of colored fabrics reveals that the highest extent of decolorization and decomposition of methylene blue occurred on fabrics coated with TiO_2 nanoparticles synthesized with 3 mL of TTIP precursor. The reflectance spectra were recorded for selected samples of fabrics dyed with methylene blue after the fabrics were exposed to UV light, and their decoloration rate was compared with their corresponding ultraviolet visible reflectance spectra.

By studying the reflectance spectrum of the raw fabric and that of two fabric samples loaded with TiO_2 nanoparticles (3 mL for each precursor) dyed with methylene blue (Fig. 16), it is observed that after 12 hours UV exposure, in the wavelength range of 600-700 nm, the raw blue fabric has the least reflection, which means that the absorption is higher in this area and the fabric is darker. Meanwhile, the reflection factor the fabrics treated with 3 mL of TTIP precursor is higher than that of its counterpart, treated with 3 mL of TTIB precursor, meaning that the self-cleaning property of the TiO_2 nanoparticles prepared from TTIP precursor is higher.

By comparing the reflectance spectra of fabrics loaded with TiO_2 nanoparticles synthesized with different concentrations of precursors, it is found that the reflection in the wavelength range of 600-700 nm is less intense in the case of the 2 mL concentration, compared to that of 3 mL for both precursors. Thus, the fabrics treated with TiO_2 nanoparticles synthesized with lower concentrations of precursor, are darker, they have higher absorption and less discoloration (Fig. 17).

CONCLUSION

In this study, titanium dioxide nanoparticles were simultaneously sonosynthesized and coated on cotton fabric. The self-cleaning properties of

cotton fabrics coated with titanium dioxide (TiO_2) nanoparticles synthesized using two different precursors: titanium isopropoxide (TTIP) and titanium butoxide (TTIB) were then investigated. The following conclusions can be drawn from the results.

The anatase phase formation of the nanoparticles with the tetragonal crystal structure was confirmed by XRD analysis. From the obtained SEM and FESEM images, it was observed that the nanoparticles are spherical and have an almost uniform distribution on the surface of the fabric. The changes in concentration and the precursor did not cause much difference in the size of the nanoparticles obtained.

The TiO_2-coated fabrics exhibited significant photocatalytic self-cleaning properties. UV-Vis spectroscopy results demonstrated that the fabrics treated with TiO_2 nanoparticles effectively degraded methylene blue, with the TTIP TiO_2-coated fabrics showing slightly better performance compared to those treated with TTIB. The photocatalytic efficiency was directly related to the concentration of the precursor used, with higher concentrations resulting in more effective self-cleaning properties.

Fabrics treated with TTIP TiO_2 nanoparticles showed superior stain removal properties, compared to those treated with TTIB TiO_2 nanoparticles.

In summary, TiO_2 nanoparticles synthesized using TTIP and TTIB precursors can effectively impart self-cleaning properties to cotton fabrics. The choice of precursor and its concentration play a crucial role in determining the efficiency of the self-cleaning effect.

ACKNOWLEDGEMENT: Authors are thankful to Rajamangala University of Technology Phra Nakhon (RMUTP), Thailand, for supporting this research.

REFERENCES

[1] S. Samal, P. Jeyaraman and V. Vishwakarma, *J. Miner. Mater. Charact. Eng.*, **9**, 519 (2010), https://file.scirp.org/pdf/JMMCE20100600002_52550434.pdf

[2] M. Bickel and C. Som, "Nano Textiles – Grundlagen und Leitprinzipienzureffizienten Entwicklungnachhaltiger Nanotextilien", TVS Textilverband Schweiz, Gallen, 2011

[3] S. T. Navale, V. V. Jadhav, K. K. Tehare, R. U. R. Sagar, C. S. Biswas *et al*., *Sensors Actuat*., **238**, 1102 (2017), https://doi.10.1016/j.snb.2016.07.136

[4] *P. Zhu, M. Wang, Z. Qiang, J. Song, Y. Wang* et al., Chem. Eng. J., ***406***, *127 (2021), https://doi.org/10.1016/j.cej.2020.127140*

[5] M. Abid, S. Bouattour, A. M. Ferraria, D. S. Conceição, A. P. Carapeto *et al*., *J. Colloid Interface Sci*., **507**, 83 (2017), https://doi.org/10.1016/j.jcis.2017.07.109

[6] Y. W. H. Wong, C. W. M. Yuen, M. Y. S. Leung, S. K. A. Ku and H. L. I. Lam, *AUTEX Res. J*., **6**, 1 (2006), https://www.infona.pl/resource/bwmeta1.element.baztech-b1b1274f-d779-4a08-87c8-94750dd28d5f

[7] A. Fujishima and X. Zhang, *C. R. Chim*., **9**, 750 (2006), https://doi.org/10.1016/j.crci.2005.02.055

[8] F. Parrino, F. R. Pomilla, G. Camera-Roda, V. Loddo and L. Palmisano, in "Titanium Dioxide (TiO_2) and Its Applications, Metal Oxides", edited by F. Parrino and L. Palmisano, 2021, Amsterdam, Elsevier Inc., 13, https://doi.org/10.1016/C2019-0-01050-3

[9] A. Kantouch, A. Bendak and M. Sadek, *Text. Res. J*., **48**, 619 (1978), https://doi.org/10.1177/0040517578048011

[10] A. Fujishima, T. N. Rao and D. A. Tryk, *J. Photochem. Photobiol. C*, 1, **1** (2000), https://doi.org/10.1016/S1389-5567(00)00002-2

[11] M. M. Karkare, *Int. Nano Lett*., **4**, 1, (2014), https://doi.org/10.1007/s40089-014-0111-x

[12] K. S. Suslick, in *Procs. 1997 IEEE Ultrasonics Symposium* (Cat. No. 97CH36118), Toronto, ON, Canada, 1997, vol. 1, p. 523, https://doi.org/10.1109/ULTSYM.1997.663076

[13] K. Yasui, T. Tuziuti, M. Sivakumar and Y. Iida, *J. Chem. Phys*., **122**, 1 (2005), https://doi.org/10.1063/1.1925607

[14] G. Marcì, E. I. García-López, L. Palmisano, D. Carriazo, C. Martín *et al*., *Appl. Catal. B*: *Environ*., **90**, 497 (2009), https://doi.org/10.1016/j.apcatb.2009.03.034

[15] J. Yang, S. Mei and J. M. F. Ferreira, *Mater. Sci. Eng. C*., **15**, 183 (2001), https://doi.org/10.1016/S0928-4931(01)00274-0

[16] A. V. Murugan, V. Samuel and V. Ravi, *Mater. Lett*., **60**, 479 (2006), https://doi.org/10.1016/j.matlet.2005.09.017

[17] P. Billik and G. Plesch, *Scrip. Mater*., **56**, 979 (2007), https://doi.org/10.1016/j.scriptamat.2007.01.048

[18] M. H. Entezari, M. Mostafai and A. Sarafraz-Yazd, *Ultrason. Sonochem*., **13**, 47 (2006), https://doi.org/10.1016/j.ultsonch.2004.12.002

[19] K. S. Kim and T. H. Kim, *J. Appl. Phys*., **125**, 070901-1 (2019), https://doi.org/10.1063/1.5060977

[20] J. H. Yu, S. Y. Kim, J. S. Lee and K. H. Ahn, *J. Nanomater*., **12**, 199 (1999), https://doi.org/10.1016/S0965-9773(99)00098-7

[21] G. Chen, G. Luo, X. Yang, Y. Sun and J. Wang, *Mater. Sci. Eng. A*, **380**, 320 (2004), https://doi.org/10.1016/j.msea.2004.03.066